THE UNIVERSITY OF WARWICK

warwickpublicationswrap

highlight your research

Post-common envelope binaries from SDSS – XVI. Long orbital period systems and the energy budget of common envelope evolution

A. Rebassa-Mansergas,[1]⋆ M. Zorotovic,[1] M. R. Schreiber,[1] B. T. Gänsicke,[2]
J. Southworth,[3] A. Nebot Gómez-Morán,[4] C. Tappert,[1] D. Koester,[5] S. Pyrzas,[2]
C. Papadaki,[6] L. Schmidtobreick,[7] A. Schwope[8] and O. Toloza[1]

[1]*Departamento de Física y Astronomía, Universidad de Valparaíso, Avenida Gran Bretana 1111, Valparaíso, Chile*
[2]*Department of Physics, University of Warwick, Coventry CV4 7AL*
[3]*Astrophysics Group, Keele University, Staffordshire ST5 5BG*
[4]*CNRS, Observatoire Astronomique, 11 rue de l'Universite, F-67000 Strasbourg, France*
[5]*Institut für Theoretische Physik und Astrophysik, University of Kiel, 24098 Kiel, Germany*
[6]*Institute of Astronomy and Astrophysics, National Observatory of Athens, 15236 Athens, Greece*
[7]*European Southern Observatory, Alonso de Cordova 3107, Santiago, Chile*
[8]*Astrophysikalisches Institut Potsdam, An der Sternwarte 16, D-14482 Potsdam, Germany*

ABSTRACT

Virtually all close compact binary stars are formed through common envelope (CE) evolution. It is generally accepted that during this crucial evolutionary phase a fraction of the orbital energy is used to expel the envelope. However, it is unclear whether additional sources of energy, such as the recombination energy of the envelope, play an important role. Here we report the discovery of the second and third longest orbital period post-common envelope binaries (PCEBs) containing white dwarf (WD) primaries, i.e. SDSS J121130.94−024954.4 ($P_{\rm orb}$ = 7.818 ± 0.002 d) and SDSS J222108.45+002927.7 ($P_{\rm orb}$ = 9.588 ± 0.002 d), reconstruct their evolutionary history and discuss the implications for the energy budget of CE evolution. We find that, despite their long orbital periods, the evolution of both systems can still be understood without incorporating recombination energy, although at least small contributions of this additional energy seem to be likely. If recombination energy significantly contributes to the ejection of the envelope, more PCEBs with relatively long orbital periods ($P_{\rm orb} \gtrsim$ 1–3 d) harbouring massive WDs ($M_{\rm wd} \gtrsim 0.8\,{\rm M_\odot}$) should exist.

Key words: stars: AGB and post-AGB – binaries: close – binaries: spectroscopic – stars: evolution – stars: low-mass – white dwarfs.

1 INTRODUCTION

Some of the most interesting objects in our Galaxy are close compact binary stars, such as cataclysmic variables, low-mass X-ray binaries or double degenerate white dwarf (WD) binaries. The vast majority of close compact binaries form through common envelope (CE) evolution occurring when the more massive star of the initial main-sequence binary fills its Roche lobe on the first giant branch (FGB) or on the asymptotic giant branch (AGB). This may trigger dynamically unstable mass transfer causing the giant's envelope to engulf its core (the future compact object) and the main-sequence companion. Drag forces transfer orbital energy and angular momentum from the binary orbit to the envelope, reducing the binary separation, until eventually the envelope is expelled and a short

orbital period post-common envelope binary (PCEB) consisting of a compact object and a main-sequence companion is exposed.

A commonly used method to predict the outcome of binary star evolution and to theoretically investigate close compact binary star populations is binary population synthesis (BPS) studies which have been performed e.g. for Type Ia supernova progenitors (Han & Podsiadlowski 2004), short gamma-ray bursts (Belczynski et al. 2006) or Galactic WD plus main-sequence (WDMS) binaries (Willems & Kolb 2004; Davis, Kolb & Willems 2010). However, in current BPS models CE evolution is commonly approximated by a parametrized energy equation, i.e. a fraction of the available orbital energy, known as the CE efficiency ($\alpha_{\rm CE}$), is equated to the binding energy of the envelope (Paczynski 1976; Webbink 1984; Iben & Tutukov 1986; Iben & Livio 1993). While recent observational as well as theoretical results indicate rather small efficiencies for the use of orbital energy, i.e. $\alpha_{\rm CE} \sim 0.25$ (Zorotovic et al. 2010; Ricker & Taam 2012), it remains unclear if, and to what extent, additional energy sources play an important role in unbinding the envelope.
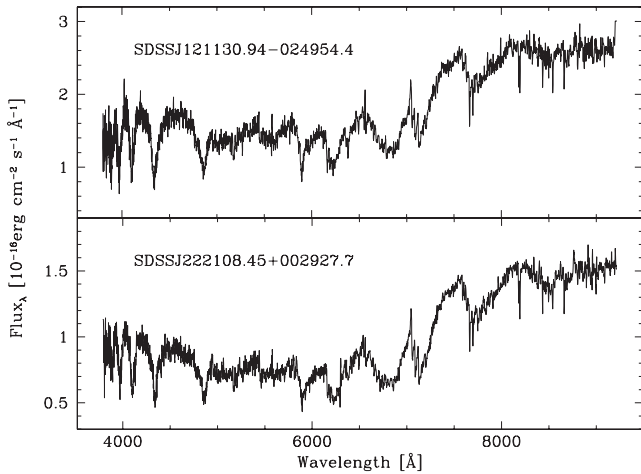
⋆E-mail: arebassa@dfa.uv.cl

Figure 1. SDSS spectra of SDSS J1211−0249 and SDSS J2221+0029.

On the one hand, the long orbital period PCEB IK Peg (Landsman, Simon & Bergeron 1993; Vennes, Christian & Thorstensen 1998) and perhaps also the two symbiotic systems T CrB (Webbink 1976) and RS Oph (Livio, Truran & Webbink 1986) have been claimed to provide direct evidence for additional energy contributions (Davis et al. 2010; Zorotovic et al. 2010), and atomic recombination is often considered to be the most promising candidate (e.g. Webbink 2008). On the other hand, Soker & Harpaz (2003) argue that recombination energy cannot significantly contribute to the ejection process as, according to them, the opacity in the envelope is too small and the energy provided by recombination should be radiated away rather than accelerating the gas.

During the last few years we have successfully identified a large number of PCEBs among WDMS binaries discovered by the Sloan Digital Sky Survey (SDSS; Adelman-McCarthy et al. 2008; Abazajian et al. 2009) and measured the orbital periods of 58 systems (Schreiber et al. 2010; Nebot Gómez-Morán et al. 2011; Rebassa-Mansergas et al. 2011). So far we have found not a single system providing additional direct evidence for recombination energy to be important. As a continuation of this large-scale project, we here present orbital period measurements of the PCEBs SDSS J121130.94−024954.4 and SDSS J222108.45+002927.7 (hereafter SDSS J1211−0249 and SDSS J2221+0029, see their SDSS spectra in Fig. 1) and find these two systems to be the longest orbital period PCEBs in our sample, and currently the second and third longest WDMS PCEBs known after IK Peg. We discuss the implications of these findings for theories of CE evolution with particular emphasis on the possible contributions of recombination energy to the energy budget of CE evolution.

2 OBSERVATIONS

We start with a brief summary of the performed spectroscopic follow-up observations of SDSS J1211−0249 and SDSS J2221+0029. Instrumentation, data reduction and calibration procedures are identical to those described in Nebot Gómez-Morán et al. (2011). A log of the observations is provided in Table 1.

2.1 SDSS J1211−0249

SDSS J1211−0249 was identified as a PCEB by Nebot Gómez-Morán et al. (2011) based on three Na I λλ8183.27, 8194.81 absorption doublet radial velocity (RV) measurements from GMOS

Table 1. Log of the observations. Provided are the telescopes and instruments used and the observing dates (observing periods are provided for the GS and VLT telescopes). The corresponding NTT ESO programme ID is 082.D-507(B).

Object SDSSJ	Telescope	Instrument	Date or observing period
1211−0249	GS	GMOS	2008 A and B
	NTT	EFOSC	2009 March 17–25
	M.Baade	IMACS	2009 May 14–16
	M.Baade	IMACS	2009 December 26–29
	VLT	FORS2	085.D-0974(A) (2010)
	VLT	FORS2	087.D-0721(A) (2011)
2221+0029	VLT	FORS2	080.D-0407(A) (2007)
	WHT	ISIS	2008 July 5–10
	CA3.5	TWIN	2008 July 25–28
	CA3.5	TWIN	2009 September 24–25
	VLT	FORS2	085.D-0974(A) (2010)
	VLT	FORS2	087.D-0721(A) (2011)

spectra taken at Gemini South (GS) during the semesters 2008 A and B. Additional follow-up spectroscopy aiming to determine the orbital period of SDSS J1211−0249 was performed at the New Technology Telescope (NTT) equipped with EFOSC during eight consecutive nights. We took a total of 18 spectra providing RVs with rather large uncertainties ($\sim$20–30 km s^{-1}) due to relatively poor weather conditions. This first data set revealed long-term RV variations for SDSS J1211−0249. Additional follow-up spectroscopy was performed at Magellan/Baade armed with IMACS during two runs of three and four nights, respectively, resulting in five additional RVs revealing a promising orbital period estimate of about 7 d. However, several aliases resulting from integer multiples of a day did not allow a definite determination of the orbital period. Finally, service mode observations at the Very Large Telescope (VLT) UT 1 equipped with FORS2 in periods 85 and 87 provided 14 additional RVs spanning the entire semesters which broke the alias degeneracy and allowed us to accurately measure the orbital period.

2.2 SDSS J2221+0029

Based on two spectra obtained with VLT/FORS2 during period 80 we discovered the close binary nature of SDSS J2221+0029 (Nebot Gómez-Morán et al. 2011). A first attempt to measure the orbital period was performed with ISIS mounted at the William Herschel Telescope (WHT), where we obtained six spectra. Given the long-term trend revealed by the RVs derived from these WHT spectra, we obtained seven additional spectra during two observing runs at the 3.5-m telescope at Calar Alto (CA 3.5) equipped with TWIN. However, as in the case of SDSS J1211−0249, the short time-span of our visitor mode observations provided multiple choices for the orbital period of SDSS J2221+0029. We hence obtained service mode observations (20 spectra) at the VLT/FORS2 during periods 85 and 87 that finally allowed us to unambiguously determine the orbital period of SDSS J2221+0029.

3 ORBITAL PERIODS

The data described in Section 2 allow us to accurately determine the orbital periods of SDSS J1211−0249 and SDSS J2221+0029. RVs were measured in all cases from the Na I λλ8183.27, 8194.81 absorption doublet, in the same fashion as described in

Table 2. Na I RVs and their errors (RVe) measured for SDSS J1211−0249 and SDSS J2221+0029. Heliocentric Julian dates (HJD) are also provided. The RVs are given in km s^{-1}.

HJD	RVs	RVe	HJD	RVs	RVe	HJD	RVs	RVe	HJD	RVs	RVe	HJD	RVs	RVe
SDSS J1211−0249														
245 4510.792 206	72.5	5.6	245 4642.555 408	33.0	5.7	245 4644.539 962	81.7	6.6	245 4911.808 350	45.1	14.1	245 4915.737 374	28.6	14.9
245 4966.586 407	27.5	8.9	245 4967.523 802	29.7	7.7	245 4967.671 370	−11.7	8.6	245 5192.758 500	39.9	11.4	245 5195.755 007	9.2	11.9
245 5287.587 077	17.2	4.8	245 5289.592 162	−16.9	5.0	245 5291.642 618	38.1	4.6	245 5293.515 465	75.1	7.5	245 5295.568 011	12.8	5.2
245 5297.512 659	−6.2	6.1	245 5299.628 209	47.6	5.1	245 5306.504 832	19.4	5.9	245 5660.552 464	89.4	11.5	245 5665.519 683	−3.7	6.8
245 5671.572 157	−5.5	5.9	245 5674.596 450	49.1	5.1	245 5677.712 572	57.5	5.2	245 5704.665 357	3.7	12.6			
SDSS J2221+0029														
245 4386.661 042	27.8	4.5	245 4387.598 545	2.2	5.3	245 4653.712 600	8.7	7.2	245 4654.647 388	0.5	8.7	245 4654.719 920	0.1	7.1
245 4655.676 768	0.5	6.6	245 4656.622 337	−7.2	7.6	245 4658.677 219	−3.7	5.9	245 5329.885 273	−0.1	8.3	245 5334.874 227	3.2	6.0
245 5344.812 435	6.9	7.6	245 5346.823 441	2.9	13.2	245 5346.834 686	−1.7	10.0	245 5346.851 469	0.7	11.3	245 5346.862 695	−6.1	11.3
245 5354.846 936	8.0	5.3	245 5357.851 973	−9.5	5.0	245 5359.794 378	−4.3	5.5	245 5360.805 659	−9.0	7.6	245 5382.720 068	6.1	6.4
245 5385.783 274	−6.3	5.0	245 5399.671 028	−2.9	8.5	245 5699.895 126	0.4	6.1	245 5711.878 306	−5.4	9.2	245 5720.842 993	−5.4	9.0
245 5724.834 694	−8.9	5.8	245 5736.779 456	4.4	6.5	245 5741.903 011	−7.9	5.9	245 4672.643 400	0.8	13.7	245 4673.556 708	1.2	10.4
245 4674.577 014	7.5	10.7	245 4675.442 195	−4.3	17.5	245 4675.641 213	−7.4	6.3	245 5099.432 743	−2.0	7.1	245 5100.353 820	−9.5	8.8

Rebassa-Mansergas et al. (2008) and Schreiber et al. (2008). The measured RVs are given in Table 2.

A Scargle (1982) periodogram calculated from the RVs of SDSS J1211−0249 to investigate the periodic nature of the velocity variations contained a number of aliases due to the sampling pattern of the visitor mode observations. Using the ORT/TSA command in MIDAS, which folds and phase-bins the data using a grid of trial periods and fits a series of Fourier terms to the folded RV curve (Schwarzenberg-Czerny 1996), we produced the periodogram shown in the top panel of Fig. 2 which reveals a clear peak at 0.128 d^{-1}. The same method applied to the RVs of SDSS J2221+0029 yields a periodogram with a clear peak at 0.104 d^{-1} (top panel of Fig. 3).

To obtain a definite value for the orbital periods we finally carried out sine fits of the form

$$V_{\mathrm{r}} = K_{\mathrm{sec}} \sin\left[\frac{2\pi(t - T_0)}{P_{\mathrm{orb}}}\right] + \gamma \qquad (1)$$

to the RV data sets, where γ is the systemic velocity, K_{sec} is the RV semi-amplitude of the companion star, T_0 is the time of inferior conjunction of the secondary star and P_{orb} is the orbital period. We
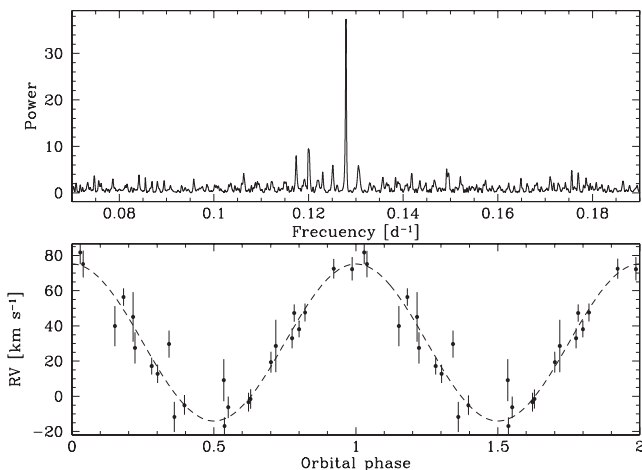

Figure 2. Top panel: ORT/TSA periodogram obtained from the RV data of SDSS J1211−0249 in Table 2. A clear peak at 0.128 d^{-1} can be seen. Bottom panel: the RV curve folded over the period provided by the periodogram in the top panel.
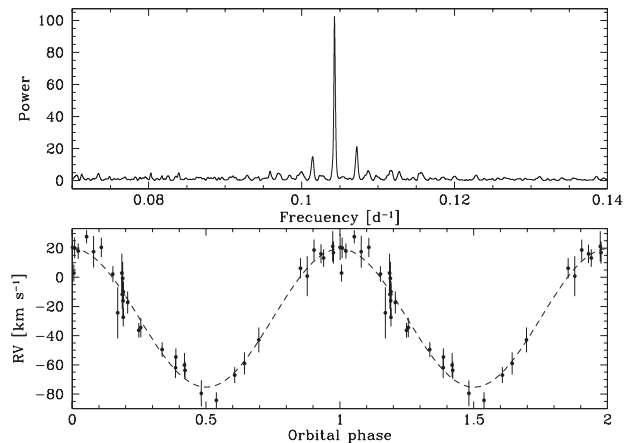

Figure 3. Top panel: ORT/TSA periodogram obtained from the RV data of SDSS J2221+0029 in Table 2. A clear peak at 0.104 d^{-1} can be seen. Bottom panel: the RV curve folded over the period provided by the periodogram in the top panel.

adopted the frequency corresponding to the strongest peaks in the periodograms as the initial orbital period. The parameters resulting from these fits are reported in Table 3 with the orbital periods of SDSS J1211−0249 and SDSS J2221+0029 being 7.818 ± 0.002 and 9.588 ± 0.002 d, respectively. These are the longest orbital periods measured so far in our survey.

4 BINARY PARAMETERS

We provide in this section the binary (orbital and stellar) parameters of the two PCEBs studied in this work. The WD effective temperatures ($T_{\mathrm{eff(WD)}}$), surface gravities ($\log g_{\mathrm{(WD)}}$) and masses (M_{wd}), as well as the secondary star spectral types (Sp$_{\mathrm{sec}}$), masses and radii (M_{sec}, R_{sec}) are obtained following the decomposition/fitting technique described in Rebassa-Mansergas et al. (2007). In brief this routine follows a two-step procedure. First, the SDSS spectrum is fitted with a two-component model, and the spectral type of the secondary star is determined (Fig. 4). Secondly, the best-fitting M dwarf is subtracted and the residual WD spectrum is fitted with a model grid of DA WDs (Koester 2010) to determine the WD effective temperature and surface gravity (Fig. 5). From an empirical spectral type radius–mass relation for M dwarfs (Rebassa-Mansergas

Table 3. Binary parameters obtained for SDSS J1211−0249 and SDSS J2221+0029. M_{wd}, M_{sec}, R_{sec}, spectral type of the companion Sp_{sec}, $T_{eff(WD)}$ and $\log g$ are obtained following the decomposition/fitting routine described in Rebassa-Mansergas et al. (2007). The orbital period P_{orb}, the secondary star semi-amplitude K_{sec} and the systemic velocity γ_{sec} are measured in Section 3. Estimates of the orbital separation a, mass ratio q, WD semi-amplitude velocity K_{wd}, secondary Roche lobe radius R_{Lsec} and inclination are obtained from the equations given in Section 4.

	SDSS J1211−0249	SDSS J2221+0029
M_{wd} (M$_\odot$)	0.52 ± 0.07	0.54 ± 0.03
M_{sec} (M$_\odot$)	0.41 ± 0.05	0.38 ± 0.07
q	0.79 ± 0.15	0.70 ± 0.15
a (R$_\odot$)	16.2 ± 0.5	18.5 ± 0.5
P_{orb} (d)	7.818 ± 0.002	9.588 ± 0.002
γ_{sec} (km s^{-1})	30 ± 2	−29 ± 2
K_{sec} (km s^{-1})	44 ± 3	49 ± 2
K_{wd} (km s^{-1})	35 ± 7	34 ± 7
Sp_{sec}	M2.5 ± 1	M3 ± 0.5
R_{sec} (R$_\odot$)	0.42 ± 0.05	0.39 ± 0.08
R_{sec}/R_{Lsec}	0.07 ± 0.01	0.06 ± 0.01
i (°)	49 ± 7	58 ± 7
$T_{eff(WD)}$ (K)	13 130 ± 860	18 440 ± 150
$\log g_{(WD)}$	7.84 ± 0.13	7.85 ± 0.06

et al. 2007) and a mass–radius relation for WDs (Bergeron, Wesemael & Beauchamp 1995; Fontaine, Brassard & Bergeron 2001) we then calculate the mass and radius of the secondary star and the WD, respectively.

For the majority of SDSS PCEBs the spectroscopic decomposition results in an uncertainty of the spectral type of ±0.5 spectral classes (Rebassa-Mansergas et al. 2010, 2012), and this also applies to SDSS J2221+0029. However, the SDSS spectrum of SDSS J1211−0249 suffers from low-frequency structure (there is substantial structure left in the residual WD spectrum after the decomposition) that results in a substantially larger uncertainty in the determination of the spectral type of the companion, and correspondingly larger uncertainties in the WD parameters (see the left-hand panels of Fig. 5 and Table 3). For SDSS J2221+0029, M_{wd},

$T_{eff(WD)}$, $\log g_{(WD)}$, M_{sec} and Sp_{sec} are obtained by averaging the fit results of two independent SDSS spectra, and the uncertainties are the corresponding standard deviations. For SDSS J1211−0249, we average the parameters over two possible solutions for the spectral decomposition using either an M2 or M3 template, and determine the uncertainties again from the corresponding standard deviations.

To calculate the binary inclinations we use Kepler's third law,

$$\frac{(M_{wd} \sin i)^3}{(M_{wd} + M_{sec})^2} = \frac{P_{orb} K_{sec}^3}{2\pi G}, \tag{2}$$

rewritten as

$$\sin i = \frac{K_{sec}}{M_{wd}} \left(\frac{P_{orb}}{2\pi G} \right)^{1/3} (M_{wd} + M_{sec})^{2/3}, \tag{3}$$

with the orbital periods and semi-amplitude velocities of the companions K_{sec} as determined in Section 3, and the stellar masses as obtained from the analysis of the SDSS spectra outlined above. The well-known relation $M_{sec}/M_{wd} = K_{wd}/K_{sec} = q$ provides an estimate of the expected semi-amplitude velocity of the WD, K_{wd}. Finally, estimates of the orbital separations and Roche lobe radii of the secondary stars R_{Lsec} are obtained from Kepler's third law and Eggleton's (1983) expression

$$R_{Lsec} = \frac{a\, 0.49\, q^{2/3}}{0.6\, q^{2/3} + \ln(1 + q^{1/3})}, \tag{4}$$

respectively. The complete sets of binary parameters for SDSS J1211−0249 and SDSS J2221+0029 are given in Table 3.

5 DISCUSSION

We have presented in the previous sections the discovery of the second and third longest orbital period (detached) PCEBs containing a WD primary. In what follows we reconstruct the evolutionary history of both systems and discuss implications for our understanding of CE evolution.

5.1 The evolution of SDSS J1211−0249 and SDSS J2221+0029

Having at hand the orbital periods, the stellar mass estimates of both components and the WD effective temperatures allow us to reconstruct the evolutionary history of SDSS J1211−0249 and
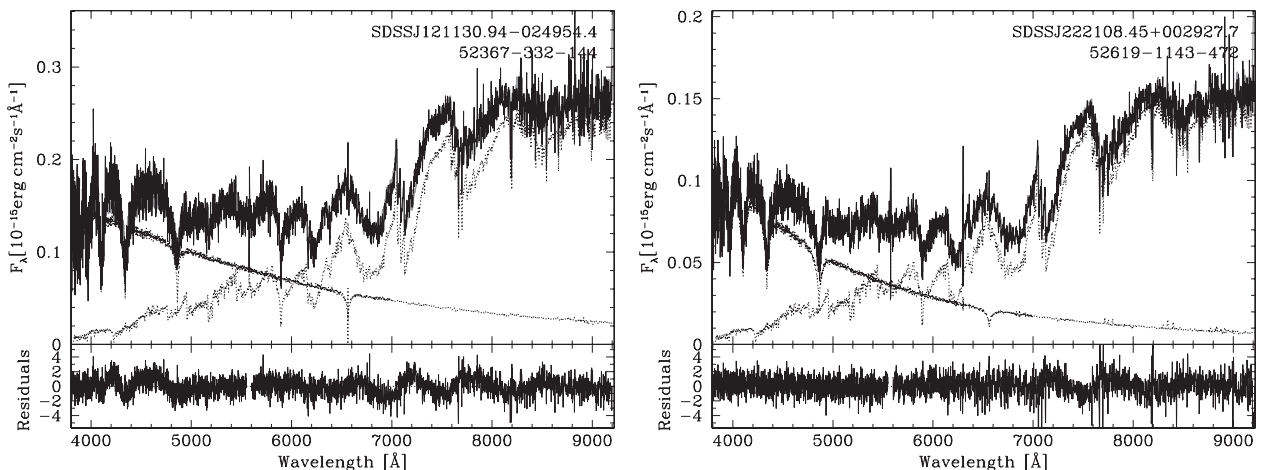

Figure 4. Two-component fit to the spectra of SDSS J1211−0249 (left) and SDSS J2221+0029 (right). The top panels show the spectra of the objects as a solid black lines and the two templates, WD and M dwarf, as dotted lines. The bottom panel shows the residuals from the fit. SDSS MJD, PLT and FIB identifiers are also indicated.
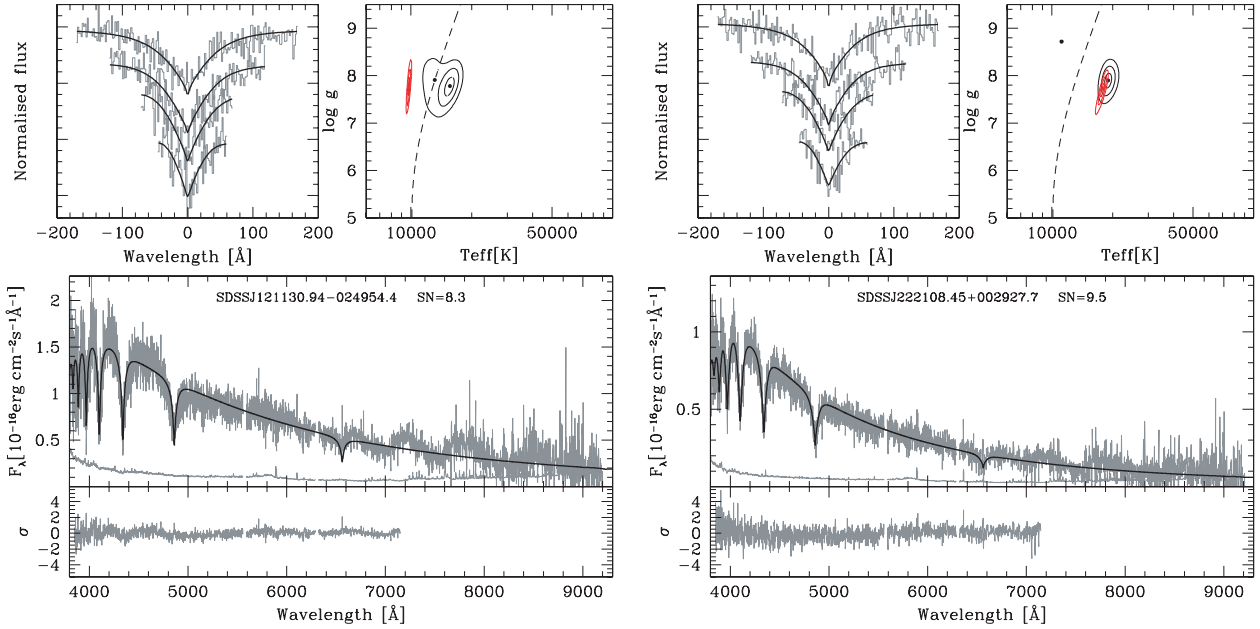
Figure 5. Spectral model fit to the WD in SDSS J1211−0249 and SDSS J2221+0029, obtained after subtracting the best-fitting M-dwarf templates (see Fig. 4). Top-left panels: best fit (black lines) to the observed Hβ to Hϵ (grey lines, top to bottom) line profiles. The model spectra and observations have been normalized in the same way. Top-right panels: 1, 2 and 3σ contour plots in the $T_{\rm eff}$–log g plane. The black contours refer to the best line profile fit, and the red ones (which collapse into a dot on the scale of the plot) to the fit of the spectral range 3850–7150 Å. The dashed line indicates the occurrence of maximum Hβ equivalent width. The best 'hot' and 'cold' line profile solutions are indicated by black dots, while the best fit to the whole spectrum by a red one. Bottom panels: the residual WD spectra resulting from the spectral decomposition and their flux errors (grey lines) along with the best-fitting WD model (black lines) in the 3850–7150 Å wavelength range (top) and the residuals of the fit (grey line, bottom).

SDSS J2221+0029 and predict their future following Zorotovic, Schreiber & Gänsicke (2011) and Schreiber & Gänsicke (2003), respectively. First, we interpolate the cooling tracks of Wood (1995) and Althaus & Benvenuto (1997) to determine the cooling age of both systems. Secondly, we derive the orbital period at the end of the CE phase using the most up-to-date version of disrupted magnetic braking (Hurley, Tout & Pols 2002, including the normalization provided by Davis et al. 2008). Thirdly, we use the single-star evolution (SSE) code of Hurley, Pols & Tout (2000) to reconstruct the CE phase for a given value of the CE efficiency and obtain the orbital and stellar parameters prior to CE evolution.

We here follow Zorotovic et al. (2010) and *assume* that recombination energy contributes to expelling the envelope with the same efficiency as the orbital energy (given by $\alpha_{\rm CE}$) and take into account the uncertainties in the stellar component masses and WD effective temperatures. We obtain solutions for rather large ranges of the CE efficiency for both systems that are given together with the resulting range of possible parameters and evolutionary time-scales of the progenitor system in Table 4. As outlined in the introduction, there seems to be some evidence for a relatively small CE efficiency and we therefore additionally provide the progenitor parameters assuming $\alpha_{\rm CE} = 0.25$ in Table 4 (the uncertainties of the stellar masses and WD effective temperature are not considered here). This complements the results presented in Zorotovic et al. (2011) (their table 3). Given that magnetic braking is not efficient in long orbital period systems, the current orbital periods (Table 3) are nearly identical to those at the end of the CE phase. The masses of the reconstructed progenitors for both objects are similar, which is not surprising since the available estimates of the stellar masses are quite similar too.

Since the current orbital periods of SDSS J1211−0249 and SDSS J2221+0029 are very long for PCEBs, the stellar components will not be close enough to trigger the second phase of mass trans-

Table 4. Applying the reconstruction algorithm described in Zorotovic et al. (2011) we determine the orbital periods at the end of CE evolution $P_{\rm CE}$, the initial mass of the primary $M_{1,\rm o}$, the mass of the primary at the onset of CE evolution $M_{1,\rm CE}$, the corresponding orbital separation $a_{\rm i}$, the main-sequence lifetime of the primary $t_{\rm evolv}$, the cooling age of the WD $t_{\rm cool}$ and the time until the second phase of mass transfer will occur from now on $t_{\rm sd}$ and since the progenitor main-sequence binary has formed $t_{\rm tot}$. Columns 2 and 4 correspond to a fixed value of $\alpha_{\rm CE} = 0.25$. Columns 3 and 5 give the entire range of possible solutions. Note that since disrupted magnetic braking is very inefficient for long orbital period systems, $P_{\rm CE}$ is nearly identical to $P_{\rm orb}$ in Table 3.

	SDSS J1211−0249		SDSS J2221+0029	
$\alpha_{\rm CE}$	0.25	0.03–1	0.25	0.06–1
$P_{\rm CE}$ (d)	7.820	7.819–7.822	9.589	9.588–9.589
$M_{1,\rm o}$ (M$_\odot$)	1.31	0.98–2.35	1.44	1.31–2.35
$M_{1,\rm CE}$ (M$_\odot$)	1.1	0.8–2.3	1.2	1.0–2.3
$a_{\rm i}$ (R$_\odot$)	480.8	246.2–613.9	512.2	295.5–611.3
$P_{\rm sd}$ (h)	26.0	24.0–28.2	32.0	28.9–36.0
$t_{\rm evolv}$ (Gyr)	4.82	0.95–13.29	3.53	0.95–4.82
$t_{\rm cool}$ (Gyr)	0.24	0.24–0.43	0.08	0.07–0.09
$t_{\rm sd}$ (Gyr)	225.3	140.1–339.7	268.5	150.13–454.36
$t_{\rm tot}$ (Gyr)	230.4	141.3–353.4	272.1	151.15–459.27

fer before the secondaries in both systems evolve away from the main sequence. Both secondaries will therefore fill their Roche lobes during the FGB transforming SDSS J1211−0249 and SDSS J2221+0029 into symbiotic systems with stable mass transfer from a red giant to a WD. This is supposed to happen in many Hubble times when the orbital periods have shrunk to ∼1–1.5 d.

5.2 The energy budget of CE evolution

In their review, Iben & Livio (1993) describe several energy sources apart from orbital energy that might contribute to expelling the envelope, ranging from recombination energy to dust-driven winds. Since the writing of this review, the energy equation of CE evolution in general, and especially the potential importance of recombination energy, has been a matter of debate (e.g. Han, Podsiadlowski & Eggleton 1994, 1995; Dewi & Tauris 2000; Soker & Harpaz 2003; Webbink 2008; Xu & Li 2010; Zorotovic et al. 2010; Loveridge, van der Sluys & Kalogera 2011).

In the previous section we reconstructed the evolution of the long orbital period PCEBs SDSS J1211−0249 and SDSS J2221+0029 *assuming* that recombination energy contributes to expelling the envelope with the same efficiency as the orbital energy and found large ranges of possible solutions. Here we investigate whether this assumed additional energy is a necessary ingredient to understand the evolutionary history of SDSS J1211−0249 and SDSS J2221+0029. To that end we now reconstruct the CE phase of both systems without considering recombination energy. Taking into account the uncertainty of the measured stellar parameters, we find possible progenitors for both systems without violating energy conservation, i.e. $\alpha_{CE} = 0.21-1$ for SDSS J1211−0249 and $\alpha_{CE} = 0.42-1$ for SDSS J2221+0029. We therefore conclude that the existence of the two systems does not confirm or disprove whether recombination (or any other additional) energy plays an important role during the CE phase. However, the current configuration of SDSS J2221+0029 can only be explained if a relatively large fraction of the released orbital energy contributes to envelope ejection, i.e. $\alpha_{CE} > 0.42$. This value exceeds the estimates given in the recent study of CE evolution by Zorotovic et al. (2010) that seem to converge towards a CE efficiency of $\alpha_{CE} \sim 0.25$ are being obtained also in hydrodynamical simulation studies (Passy et al. 2012; Ricker & Taam 2012). However, one should be careful when interpreting these results as observed samples are still biased and the simulations do not yet cover the entire envelope ejection process. Still, if a small value of the CE efficiency can be further confirmed, at least a small fraction of recombination energy (or any other form of additional energy) seems to have contributed to the envelope ejection in SDSS J2221+0029. Although this interpretation appears tempting, the fact remains that not a single PCEB within the homogeneous SDSS sample (Nebot Gómez-Morán et al. 2011) provides *direct* evidence for additional sources of energy playing a role during CE evolution.

5.3 Future perspectives

IK Peg has been highlighted as a key object as it is the longest orbital period system and contains the most massive secondary star among the known PCEBs containing a WD primary. IK Peg requires extra energy that helps to expel the envelope during CE evolution (e.g. Davis et al. 2010). Indeed, IK Peg cannot be reconstructed unless at least a small fraction of recombination energy is taken into account (Zorotovic et al. 2010). In contrast to IK Peg the two PCEBs discussed here, SDSS J1211−0249 and SDSS J2221+0029, contain relatively low-mass C/O-core WDs (Table 3); therefore, their progenitors filled their Roche lobes early on the AGB, i.e. when the envelope was not very extended. Recombination energy, however, is expected to be most important when the WD progenitor radius is large and the envelope is loosely bound (Webbink 2008). The peculiarity of IK Peg is therefore not only its long orbital period but also the high mass of its WD, which implies that the system
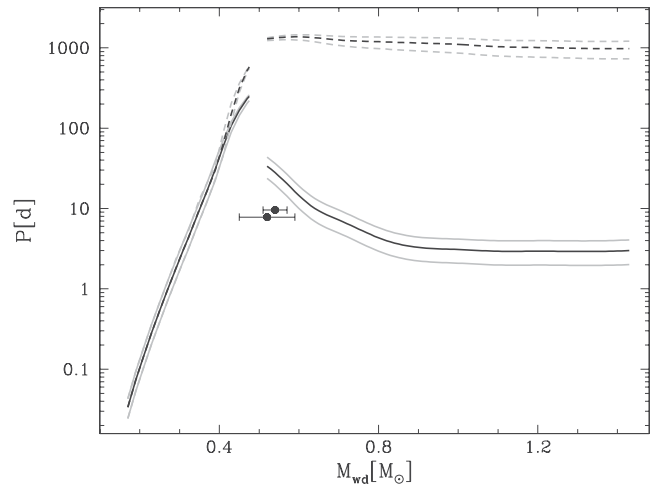

Figure 6. Maximum orbital period versus WD mass assuming a secondary star mass of $M_{sec} = 0.4$ (black lines) $\pm 0.1\,M_{\odot}$ (grey lines). The dashed lines correspond to the maximum orbital period if all recombination energy goes into CE ejection, while the solid lines provide the same limit but without taking into account possible contributions from recombination. Any system located between the two lines would provide direct evidence for the contributions of recombination energy. The difference between both lines is largest for high-mass WDs as the relative importance of recombination energy increases on the AGB. So far all PCEBs in the homogeneous SDSS sample lie well below the solid lines. Note that the exact location of the two lines depends on the secondary star mass. PCEBs with more massive secondaries have more orbital energy available and the limits are hence slightly shifted towards longer orbital periods.

entered the CE phase when the radius of the primary was very large on the AGB, a peculiarity our two PCEBs do not share.

To predict which kind of PCEBs would provide the desired direct evidence for contributions of recombination energy we once more use the reconstruction algorithm described in Zorotovic et al. (2011). As usual we assume that the WD mass is equal to the core mass of the giant progenitor at the onset of mass transfer and that the secondary star mass remains constant during CE evolution. For a given core mass we use the SSE code from Hurley et al. (2000) to calculate all possible progenitor masses and their radii. As the radius of the progenitor must have been equal to the Roche radius at the onset of CE evolution we obtain the initial separation for given WD and main-sequence companion masses, leaving the final orbital period and the CE efficiency as the remaining free parameters connected via the energy equation. For each progenitor mass the solution with $\alpha_{CE} \simeq 1.0$ corresponds to the longest possible final orbital period not violating energy conservation. Among these possible solutions we finally can select the maximum orbital period for a given combination of WD and secondary star masses.

In Fig. 6 we show the resulting PCEB maximum orbital period as a function of WD mass assuming a fixed secondary star mass of $M_{sec} = 0.4 \pm 0.1\,M_{\odot}$. The positions of SDSS J1211−0249 and SDSS J2221+0029 are indicated by black solid dots. The dashed lines have been obtained by assuming that all the available recombination energy goes into envelope ejection while the solid lines represent the maximum orbital period if the envelope is expelled by the use of orbital energy only. The upper and lower (solid and dashed) grey lines correspond to $M_{sec} = 0.5\,M_{\odot}$ and $M_{sec} = 0.3\,M_{\odot}$, respectively. The orbital period limits increase with the secondary star mass because PCEBs with more massive secondaries have more orbital energy available.

Any PCEB located above the solid line in Fig. 6 (for a given secondary star mass) would provide direct evidence for contributions of additional energy sources. Apparently, recombination energy as the most likely extra energy can only be important on the tip of the FGB and on the AGB (see the dashed lines in Fig. 6). For high-mass WDs ($M_{wd} \gtrsim 0.8\,M_\odot$) the range of orbital periods that would provide evidence for recombination energy is significantly shifted towards shorter (easily measurable) orbital periods of a few days. However, so far not a single known PCEB apart from IK Peg has a relatively long orbital period *and* contains a high-mass WD. The seven SDSS PCEBs with accurately determined orbital periods and stellar parameters containing massive WDs ($\geq 0.8\,M_\odot$) have orbital periods shorter than 1 d (see table 3 in Zorotovic et al. 2011). This might further indicate that the fraction of recombination energy going into envelope ejection is small. However, further observational constraints are required to confirm this supposition. We have therefore just started an observing campaign to measure orbital periods of additional SDSS PCEBs with $M_{wd} \gtrsim 0.8\,M_\odot$ to further constrain the importance of recombination energy during CE evolution. The secondary star masses of the PCEBs in our SDSS follow-up project are mostly in the range of $M_{sec} \sim 0.2$–$0.4\,M_\odot$ which corresponds to orbital period limits given by the full use of orbital energy of $\sim$1–3 d (see Fig. 6). Direct evidence for additional energy, most likely from recombination, would be provided if at least one system is found to have a period exceeding this limit. In contrast, if no such system is detected, the contribution of recombination energy during CE evolution is likely of minor importance.

6 CONCLUSION

We have measured the orbital periods of SDSS J1211−0249 and SDSS J2221+0029 to be 7.818 ± 0.002 and 9.588 ± 0.002 d, respectively. This makes them the longest orbital period PCEBs containing a WD primary and main-sequence companion after the well-known record holder IK Peg. We reconstructed the CE evolution of both systems taking into account and ignoring additional sources of energy. Although no direct evidence for contributions of recombination energy during CE evolution is provided, it appears plausible that at least a small fraction of this energy helped expelling the envelope. Measuring the orbital periods of more PCEBs containing high-mass ($M_{wd} \gtrsim 0.8\,M_\odot$) WDs will provide further constraints on the importance of recombination energy during CE evolution.

REFERENCES

Abazajian K. N. et al., 2009, ApJ, 182, 543
Adelman-McCarthy J. K. et al., 2008, ApJS, 175, 297
Althaus L. G., Benvenuto O. G., 1997, ApJ, 477, 313
Belczynski K., Perna R., Bulik T., Kalogera V., Ivanova N., Lamb D. Q., 2006, ApJ, 648, 1110
Bergeron P., Wesemael F., Beauchamp A., 1995, PASP, 107, 1047
Davis P. J., Kolb U., Willems B., Gänsicke B. T., 2008, MNRAS, 389, 1563
Davis P. J., Kolb U., Willems B., 2010, MNRAS, 403, 179
Dewi J. D. M., Tauris T. M., 2000, A&A, 360, 1043
Eggleton P. P., 1983, ApJ, 268, 368
Fontaine G., Brassard P., Bergeron P., 2001, PASP, 113, 409
Han Z., Podsiadlowski P., 2004, MNRAS, 350, 1301
Han Z., Podsiadlowski P., Eggleton P. P., 1994, MNRAS, 270, 121
Han Z., Podsiadlowski P., Eggleton P. P., 1995, MNRAS, 272, 800
Hurley J. R., Pols O. R., Tout C. A., 2000, MNRAS, 315, 543
Hurley J. R., Tout C. A., Pols O. R., 2002, MNRAS, 329, 897
Iben I. J., Livio M., 1993, PASP, 105, 1373
Iben I., Jr, Tutukov A. V., 1986, ApJ, 311, 742
Koester D., 2010, Mem. Soc. Astron. Ital., 81, 921
Landsman W., Simon T., Bergeron P., 1993, PASP, 105, 841
Livio M., Truran J. W., Webbink R. F., 1986, ApJ, 308, 736
Loveridge A. J., van der Sluys M. V., Kalogera V., 2011, ApJ, 743, 49
Nebot Gómez-Morán A. et al., 2011, A&A, 536, A43
Paczynski B., 1976, in Eggleton P., Mitton S., Whelan J., eds, Proc. IAU Symp. 73, Structure and Evolution of Close Binary Systems. Reidel, Dordrecht, p. 75
Passy J.-C. et al., 2012, ApJ, 744, 52
Rebassa-Mansergas A., Gänsicke B. T., Rodríguez-Gil P., Schreiber M. R., Koester D., 2007, MNRAS, 382, 1377
Rebassa-Mansergas A. et al., 2008, MNRAS, 390, 1635
Rebassa-Mansergas A., Gänsicke B. T., Schreiber M. R., Koester D., Rodríguez-Gil P., 2010, MNRAS, 402, 620
Rebassa-Mansergas A., Nebot Gómez-Morán A., Schreiber M. R., Girven J., Gänsicke B. T., 2011, MNRAS, 413, 1121
Rebassa-Mansergas A., Nebot Gómez-Morán A., Schreiber M. R., Gänsicke B. T., Schwope A., Gallardo J., Koester D., 2012, MNRAS, 419, 806
Ricker P. M., Taam R. E., 2012, ApJ, 746, 74
Scargle J. D., 1982, ApJ, 263, 835
Schreiber M. R., Gänsicke B. T., 2003, A&A, 406, 305
Schreiber M. R., Gänsicke B. T., Southworth J., Schwope A. D., Koester D., 2008, A&A, 484, 441
Schreiber M. R. et al., 2010, A&A, 513, L7
Schwarzenberg-Czerny A., 1996, ApJ, 460, L107
Soker N., Harpaz A., 2003, MNRAS, 343, 456
Vennes S., Christian D. J., Thorstensen J. R., 1998, ApJ, 502, 763
Webbink R. F., 1976, Nat, 262, 271
Webbink R. F., 1984, ApJ, 277, 355

Webbink R. F., 2008, in Milone E. F., Leahy D. A., Hobill D. W., eds, Astrophys. Space Sci. Libr., Vol. 352, Short-Period Binary Stars: Observations, Analyses, and Results. Springer Berlin, p. 233

Willems B., Kolb U., 2004, A&A, 419, 1057

Wood M. A., 1995, in Koester D., Werner K., eds, Lecture Notes in Physics, Vol. 443, White Dwarfs. Springer-Verlag, Berlin, p. 41

Xu X.-J., Li X.-D., 2010, ApJ, 716, 114

Zorotovic M., Schreiber M. R., Gänsicke B. T., Nebot Gómez-Morán A., 2010, A&A, 520, A86

Zorotovic M., Schreiber M. R., Gänsicke B. T., 2011, A&A, 536, A42

This paper has been typeset from a TEX/LATEX file prepared by the author.